





## Article

# Improving Acoustic Properties of Sandwich Structures Using Recycled Membrane and HoneyComb Composite (RMHCC)

Giuseppe Ciaburro <sup>1,\*</sup>, Virginia Puyana Romero <sup>2,\*</sup>, Gino Iannace <sup>1</sup> and Luis Bravo Moncayo <sup>2,3</sup>

<sup>1</sup> Department of Architecture and Industrial Design, University of Campania, Luigi Vanvitelli, 81031 Aversa, Italy; gino.iannace@unicampania.it

<sup>2</sup> Faculty of Engineering and Applied Sciences, Department of Sound and Acoustic Engineering, University of Las Américas, Quito 170125, Ecuador; luis.bravo.moncayo@gmail.com

<sup>3</sup> Engineering Dynamics Consultancy, Vysus Group, 2750 Ballerup, Denmark

\* Correspondence: giuseppe.ciaburro@unicampania.it (G.C.); virginiapuyana@yahoo.es (V.P.R.)

**Abstract:** The motivation behind this study is to improve acoustic environments in living spaces using sustainable materials. This research addresses the challenge of enhancing the acoustic properties of sandwich structures through the integration of a honeycomb core with a membrane made from recycled materials, forming a recycled membrane honeycomb composite (RMHCC). The main objective is to develop a novel sandwich material with sound-absorbing characteristics suitable for real-world applications. The study employs both experimental methods and simulations, where a conventional hexagonal honeycomb geometry is combined with the recycled membrane to form the composite structure. A simulation model was developed to evaluate the effectiveness of the metamaterial in reducing reverberation time within a church setting. The results indicate that the RMHCC shows significant potential in improving acoustic performance, with a notable reduction in reverberation time even with minimal usage, highlighting its suitability for enhancing acoustic environments in various applications.

**Keywords:** acoustic metamaterial; environmental sustainability; building construction; sound absorption properties; room acoustics software



**Citation:** Ciaburro, G.; Romero, V.P.; Iannace, G.; Bravo Moncayo, L. Improving Acoustic Properties of Sandwich Structures Using Recycled Membrane and HoneyComb Composite (RMHCC). *Buildings* **2024**, *14*, 2878. <https://doi.org/10.3390/buildings14092878>

Academic Editor: Francesco Nocera

Received: 26 August 2024

Revised: 9 September 2024

Accepted: 10 September 2024

Published: 12 September 2024



**Copyright:** © 2024 by the authors. Licensee MDPI, Basel, Switzerland. This article is an open access article distributed under the terms and conditions of the Creative Commons Attribution (CC BY) license (<https://creativecommons.org/licenses/by/4.0/>).

## 1. Introduction

The need to improve the acoustic properties in living environments is a question of growing importance in the contemporary context. Domestic environments, which should be places of rest and tranquility, often find themselves facing a series of challenges related to noise, which can compromise the well-being of the inhabitants. This results in the need to improve home acoustics, to mitigate the negative impact of noise on the health and comfort of individuals, with the aim of identifying solutions and technologies available to address this problem [1]. Firstly, it is important to understand the crucial role that living environments play in people's well-being. The home is the refuge where one expects to be able to relax and regenerate; however, the noise coming from various external and internal sources can compromise this experience. Traffic noise, daily activities, household appliances and even conversations can create a stressful and disturbing sound environment within the home, thereby, negatively affecting sleep, concentration and overall quality of life [2].

Secondly, numerous scientific studies have demonstrated the harmful effects of noise on physical and mental health. Excessive noise can cause stress, sleep disturbances, increased blood pressure and even heart problems [3]. Furthermore, it can negatively influence learning, productivity and emotional well-being, especially in children and the elderly. As a result, creating quiet, noise-free home environments becomes essential to promoting the overall health and well-being of the inhabitants [4]. To address this challenge, it is necessary to adopt proactive approaches to improve the acoustic properties in living environments.

There are several solutions available, ranging from the use of insulating and sound-absorbing materials to targeted architectural design. For example, installing double-glazing, soundproofing walls and using heavy carpets and curtains can help reduce noise transmission within the home [5]. At the same time, the use of advanced technologies such as active sound insulation systems and noise cancellation devices can offer effective solutions to reduce unwanted noise. Furthermore, it is important to consider the environmental impact of the solutions adopted to improve home acoustics. The use of sustainable and eco-friendly materials, such as natural insulation and recycled materials, not only help reduce noise but also promote environmental sustainability. In this context, innovation and research in the field of acoustic materials and technologies play a fundamental role in providing effective and eco-friendly solutions to improve home acoustics [6].

Sandwich structures are widely used in architecture for their versatility and performance. They offer a balance between structural resistance, thermal and acoustic insulation. The combination of insulating internal and resistant external layers allows the creation of modern buildings with high thermal and acoustic performance [7]. These structures find application in residences, commercial and industrial buildings, helping to improve user comfort and reducing the environmental impact of buildings. Sandwich structures, being made up of two rigid outer layers separated by light and thick structural material, offer a few advantages that make them particularly suitable for acoustic applications. First, the sandwich structure offers considerable mechanical resistance with low weight. This feature is fundamental for the construction of panels and walls that must withstand structural loads while minimizing the total weight of the structure itself. Furthermore, the lightness of the structure makes its installation and maintenance easier, thus helping to reduce construction costs and time [8].

Another advantage of sandwich structures is their ability to provide excellent thermal and acoustic insulation properties. The structural material located between the rigid external layers acts as an effective barrier to the passage of sound, thus reducing the transmission of noise through the structure itself. This feature is particularly advantageous in environments where it is necessary to guarantee a high level of acoustic privacy, such as offices, recording studios or conference rooms. The versatility of sandwich structures makes them suitable for a wide range of acoustic applications [9]. They can be used for the construction of partition walls, ceilings, floors and sound-absorbing panels, offering a solution tailored to the specific needs of each environment. Furthermore, the possibility of customizing the composition and thickness of the materials allows for optimal acoustic performance based on specific sound insulation and absorption needs, for example in rooms with special acoustic needs for speech intelligibility, such as churches or theaters [10]. An important aspect to consider is the design and optimization of the acoustic properties of sandwich structures. This includes choosing the appropriate materials for the outer layers and the internal structural material, as well as designing the geometry and thickness of the structure to maximize the desired acoustic performance. Modern modeling and simulation techniques allow engineers and designers to evaluate and optimize the acoustic performance of sandwich structures before physical construction, thus reducing development time and costs [11].

In this work, a sandwich sound-absorbing panel was created using a solution that incorporates membranes made from recycled materials as external structures, along with a honeycomb structure serving as the internal connective element. The motivation for using honeycomb material and recycled membrane comes from the search for sustainable and effective solutions to improve the acoustic properties of structures, while simultaneously addressing the challenges related to waste management and environmental sustainability. This combination of materials offers a series of advantages that make them particularly suitable for applications that require high acoustic performance and a reduced environmental footprint. First, honeycomb material is known for its light weight, strength and rigidity, making it a great choice for the load-bearing structure of sandwich structures [12]. Its hexagonal cell structure offers excellent energy absorption and load distribution capacity,

allowing you to create light and robust structures with a low weight. This is particularly advantageous for applications where it is necessary to maximize mechanical strength without adding additional weight to the structure, such as in the case of partition walls or suspended ceilings [13]. Li et al. [14] studied the sound insulation of functionally graded honeycomb sandwich plates and found that negative Poisson's ratio of honeycomb cores had much lower natural frequencies than conventional hexagonal cells. Scarpa et al. [15] investigated the optimization of honeycomb sandwich structures to improve blast resistance through manipulation of their negative Poisson's ratio (NPR) properties. The study investigates how modifying the structural characteristics of honeycomb sandwich panels can improve their ability to resist explosion loads. The researchers specifically explore the concept of negative Poisson's ratio, which is known to impart unique mechanical properties such as increased energy absorption and increased toughness. Through a series of experimental and numerical analyses, the authors demonstrate methods for tailoring the NPR of honeycomb sandwich structures. They examine various parameters such as cell geometry, core material properties and sandwich configuration to optimize blast resistance while maintaining structural integrity. The results highlight the potential of auxetic honeycomb cores, which have a negative Poisson's ratio, to improve blast resistance compared to conventional honeycomb structures. The study provides insights into the design principles and structural optimization techniques of honeycomb sandwich panels to mitigate the effects of explosive loading, thus contributing to advances in protective engineering applications. Li et al. [16] explored the sound insulation performance of sandwich panels with double arrowhead honeycomb cores with negative Poisson's ratio (NPR). The results showed improved vibration and acoustic attenuation behaviors and produced higher STL values compared to the optimized decreasing gradient NPR models. Therefore, sandwich panels can achieve desirable vibroacoustic performance with higher bending stiffness than traditional hexagonal honeycomb sandwich structures, and the design can be extended to achieve optimized vibration and noise control capabilities. Griese et al. [17] found that honeycomb with smaller internal cell angles improved sound transmission loss in the low frequency range. Furthermore, honeycombs with negative Poisson's ratio can be divided into reentrant structures, chiral structures, missing rib structures, and other honeycomb geometries. Meng et al. [18] propose the band gap in a much lower frequency region when the star-shaped honeycomb Poisson ratio is in negative values.

The use of recycled membrane reduces the environmental impact associated with the production and disposal of materials. Recycled membranes can be obtained from a variety of sources, such as recycled plastic bottles or industrial waste, and treated to achieve the desired properties for the specific application [19]. This approach not only reduces the amount of waste sent to landfills but also helps reduce the use of natural resources and greenhouse gas emissions associated with the production of new virgin materials [20]. The combination of honeycomb material and recycled membrane also offers high design and customization flexibility. The ability to shape and manipulate these materials allows the creation of structures with a wide range of acoustic properties, adaptable to the specific sound insulation and absorption needs of each environment. Furthermore, the availability of recycled membrane in a variety of colors and textures allows the acoustic solutions to be integrated into the overall aesthetics of the environment, ensuring a coherent and harmonious design. Another significant advantage of using recycled materials is the reduction of production and management costs. Honeycomb materials and recycled membranes tend to be cheaper than their virgin equivalents, allowing production costs to be reduced without compromising the performance or quality of the final product. Furthermore, the availability of recycled material in the market is constantly increasing; thanks to the growing awareness of the importance of environmental sustainability and the desire to reduce the environmental impact of one's activities. The use of honeycomb material and recycled membrane offers a sustainable and effective solution to improve the acoustic properties of structures, while simultaneously reducing the environmental impact resulting from the production and disposal of materials. This combination of

materials offers several advantages, including lightweight, strength, design flexibility and cost reduction, making it an attractive choice for a wide range of acoustic applications.

## 2. Materials and Methods

### 2.1. Sandwich Structure Definition

A sandwich panel is a composite structure consisting of two outer layers, or skins, enclosing a core material. These skins can be made from various materials, including metals (e.g., aluminum, steel), composites (e.g., fiberglass, carbon), polymers (e.g., thermoplastics, thermosets), or natural materials (e.g., wood, plywood) [21]. The external layers provide mechanical strength, protection from environmental factors, and aesthetic appeal [22].

In this work, a membrane was produced using recycled materials (Figure 1), specifically recycled food-grade aluminum foil and recycled polyester fibers, which were bonded together with polyurethane glue. This approach aims to reduce environmental impact and promote sustainability. This process combines advanced techniques with eco-sustainable practices to create a high-quality final product that reduces the use of virgin resources and promotes the reuse of existing materials [23].

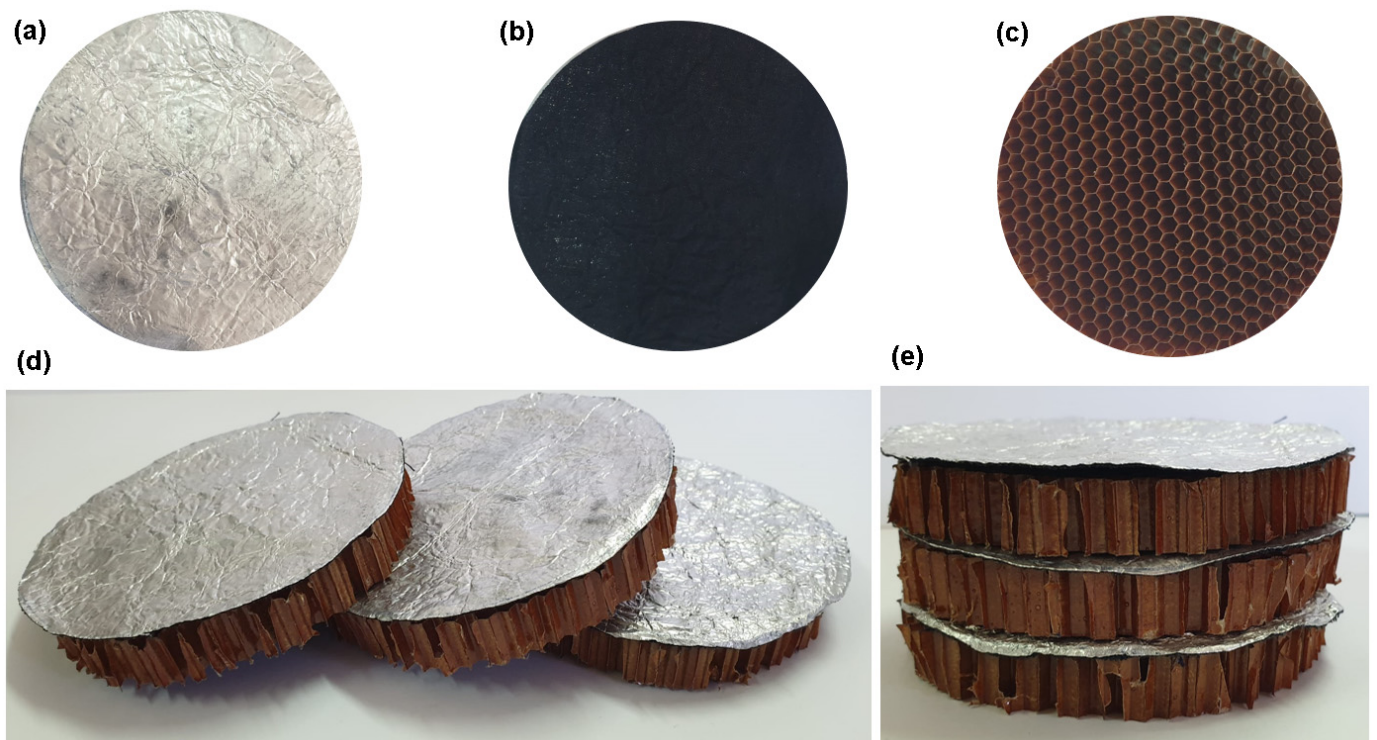


**Figure 1.** Membrane and honeycomb structure. (a) Membrane based on recycled material, aluminum film side; (b) Membrane based on recycled material, fabric side; (c) honeycomb structure; (d) Three groups of couple membrane-honeycomb; (e) Sandwich sample with three groups of couple membrane-honeycomb stacked.

The first phase of the process begins with the collection and preparation of recycled materials. Food-grade aluminum foil, from post-consumer or industrial sources, undergoes a rigorous selection and cleaning process to remove any contaminants and prepare it for reuse. Similarly, recycled polyester fibers are recovered from textile waste or old clothing, then treated and transformed into a form suitable for use. Once the materials are prepared, the processing phase begins. The aluminum foil is melted and laminated to create a uniform layer of material that will form the base of the membrane. The recycled polyester fibers, appropriately treated to improve their strength and cohesion, are then distributed across the surface of the film in a pre-determined pattern. This process requires precision and care to ensure even fiber distribution and strong adhesion to the aluminum base.

Next, polyurethane glue comes into play. This adhesive is strategically applied to the surface of the aluminum film and polyester fibers to create a cohesive and durable layer. The polyurethane glue was chosen for its excellent adhesion properties and resistance to atmospheric agents, ensuring that the final membrane is durable and reliable even in adverse environmental conditions.

The core of a sandwich panel is typically composed of lightweight, low-density materials such as polymer foams, expanded polystyrene, wood, cardboard, or honeycomb materials. This core contributes to the panel's lightness and imparts specific thermal, acoustic, and structural properties, depending on the material used. A honeycomb core, inspired by natural bee honeycombs [24], provides a balance of lightness and mechanical strength through its hexagonal or polygonal cell arrangement (Figure 1c). This structure is known for its high compressive strength and minimal material use and can be enhanced with insulating materials to improve thermal and acoustic insulation in buildings or vehicles [25]. Table 1 shows the physical properties of the materials used for the preparation of the specimens.

**Table 1.** Physical properties of the materials used for the preparation of the specimens.

Properties	Membrane	Honeycomb	Glue
Material type	aluminum–polyester	aromatic polyamide	polyurethane
Thickness (cm)	0.03	1.3	--
Radius (cm)	5	5	--
Mass (g)	2.3	3.2	--
Density (g/cm <sup>3</sup> )	0.976	0.157	1.3
Cell type	--	exagonal	--
Cell size (cm)	--	0.4	--
Void Fraction		0.8	

Honeycomb structures are highly effective in sound absorption due to several intrinsic characteristics. The honeycomb geometry creates a large contact area between cell walls, enhancing the interception and absorption of sound waves [26]. The thin walls allow sound to penetrate and be dispersed within the structure, where internal friction reduces the energy of the sound waves and decreases noise intensity [27]. The core material, often porous like polymer foams or cardboard, further dampens acoustic vibrations by converting sound energy into heat through molecular movement. Additionally, honeycomb structures can be customized in terms of density, cell size, and materials to optimize acoustic performance for specific frequencies or environments, such as recording studios or conference rooms [28]. They can also be integrated with other materials or systems, such as additional coatings or vibrational isolation systems, to further enhance their acoustic capabilities.

The peculiar shape of the honeycomb structure is the non-regular hexagon, but various unit cell designs of the honeycomb structure have been studied. Depending on the behavior of the deformation caused by the force, honeycombs can be classified as conventional hexagonal honeycombs, honeycombs with zero Poisson's ratio and honeycombs with negative Poisson's ratio effects [29]. Conventional hexagonal honeycombs are the most encountered type of honeycomb structure. As the name suggests, their individual cells are arranged in a regular hexagonal pattern. These honeycombs exhibit typical Poisson's ratio behavior under deformation, where the material contracts laterally when subjected to axial loading and vice versa. This behavior is in line with traditional expectations of material deformation. Zero Poisson's ratio honeycombs possess a unique mechanical property in which they do not undergo lateral expansion or contraction when subjected to axial loading. In a positive Poisson's ratio honeycomb structure, when the material is subjected to a deformation along one direction (for example, longitudinal stretching or compression), an opposite transverse deformation occurs [30]. This means that if the material is stretched, it contracts laterally, and if it is compressed, it expands laterally. Positive Poisson's ratio is a common characteristic in most traditional materials. These honeycombs are characterized by specialized geometries and cellular configurations that allow this behavior. They

find applications in areas where isotropic deformation properties are desired, such as in vibration damping or structures requiring greater dimensional stability. Negative Poisson's ratio honeycombs, also known as auxetic honeycombs, exhibit counterintuitive behavior in which they expand laterally when compressed axially and contract laterally when stretched axially. This inverse behavior challenges conventional principles of material deformation and is achieved through complex cell geometries and arrangements [31].

Recycled membranes and honeycomb structures were combined to create the sandwich panel. Various configurations were tested by altering the number of membrane layers and their positions to identify the most effective arrangement and optimize the panel's design. This iterative process aimed to enhance the panel's overall performance, considering factors such as acoustic properties, structural integrity, and environmental impact (Figure 2).

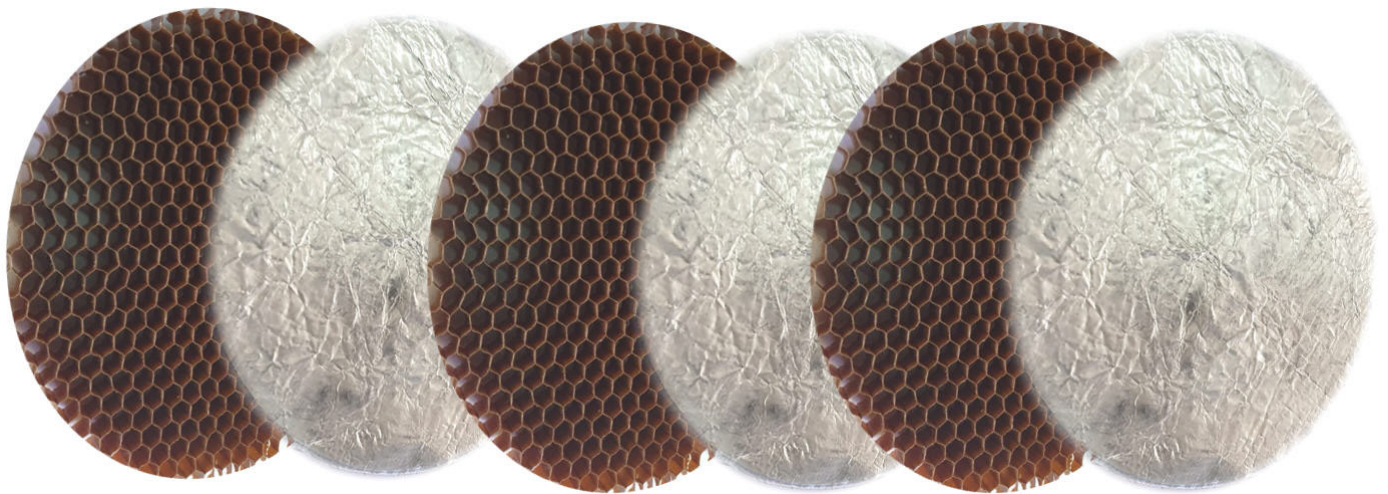


**Figure 2.** Sandwich structure with sequence of several layers of membranes and honeycomb structures.

### 2.2. Sound Adsorption Coefficient Measurements

Sound absorption coefficient (SAC) measurements were performed in accordance with ISO-10534-2:2023 [32]. These measurements are of fundamental importance for understanding the acoustic characteristics of materials. The precision and reliability of these measurements are crucial for designing environments with optimal acoustic conditions. A commonly used and widely accepted method for determining sound absorption coefficients is the use of the impedance tube, which has proven its effectiveness in multiple applications. Acoustic absorption is the phenomenon whereby a material dissipates sound energy instead of reflecting it. The sound absorption coefficient, which represents the ratio between absorbed and incident sound energy, is a fundamental parameter in numerous sectors, including architecture and automotive engineering. Understanding the interactions between materials and sound waves allows engineers to design environments with specific acoustic qualities. Measurements of these coefficients are essential for several applications, such as optimizing reverberation time in auditoriums and concert halls or developing sound-absorbing materials to improve the acoustic comfort of automotive interiors. These findings allow us to create spaces that adequately respond to the desired acoustic needs, thus improving both the auditory experience and the functionality of the environments.

The impedance tube, a classic device such as the Model SCS type 9020B/K (Figure 3), is used to measure the speed of sound in gases and to determine the acoustic properties of materials, including absorption coefficients acoustic. This instrument operates according to the principle of resonance, using a standing wave to make the material vibrate at the same frequency as the incident sound wave. ISO 10534-2:2023 specifies procedures for measuring sound absorption coefficients using impedance tubes [33]. This standard places particular emphasis on creating a controlled environment, including precise control of temperature and humidity, and the use of a reference material for calibration, to ensure

consistent and accurate measurements between different laboratories. The use of the impedance tube compliant with ISO 10534-2:2023 offers a standardized and reliable method for evaluating sound absorption coefficients, allowing consistent and precise comparisons between results obtained in different laboratories. This standard ensures that measurements are reproducible and accurate, contributing to the validity of the data collected and their applicability in fields such as architecture, civil engineering, and the automotive industry, where acoustic quality is of fundamental importance [34].

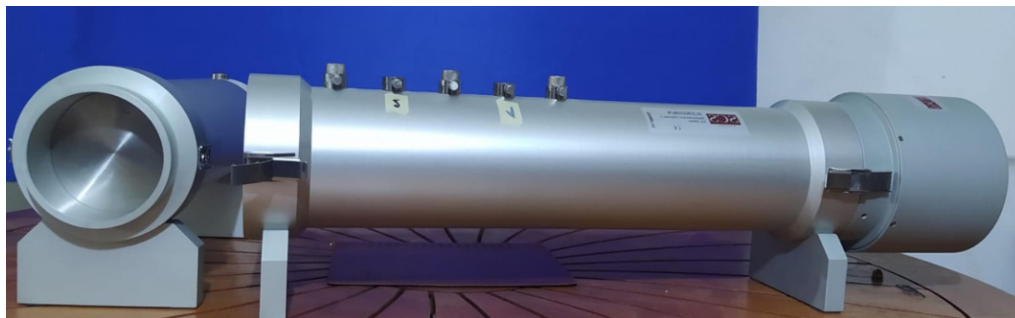


**Figure 3.** Impedance tube for measuring the absorption coefficient at normal incidence (Model SCS type 9020B/K).

Despite its robustness, the impedance tube presents some operational challenges. The choice of tube material and any issues in the tested material, such as leaks or non-uniformity, can introduce significant errors into measurements. To minimize these potential sources of error, it is essential to scrupulously follow the guidelines of ISO 10534-2:2023 and pay particular attention to experimental details.

In this study, an impedance tube with the following specifications was used: an internal diameter of 10 cm, which allows reaching an upper-frequency limit of 2000 Hz, a length of 56 cm, and two  $\frac{1}{4}$ " microphones positioned 5 cm apart to make accurate measurements above 200 Hz. These dimensions have been selected to ensure precise and reliable measurements over a wide range of frequencies. The impedance tube configuration adopted in this study was designed to cover a broad frequency spectrum, thus ensuring that the data collected is representative of the acoustic properties of the tested material. The use of two strategically positioned microphones allows the sound pressure variations to be precisely captured, helping to determine the sound absorption coefficients accurately. Through careful calibration and rigorous adherence to experimental protocols, errors can be minimized, and reliable results can be obtained that can be consistently compared across different laboratories and applications.

The thickness of the samples was 4 cm to ensure they were representative of the actual material conditions. The normal incidence sound absorption coefficient and the normal specific acoustic impedance were measured. A broadband noise source was used to generate sound waves within the tube, and the microphone positions were calibrated to capture the incident and reflected sound waves. The two-microphone transfer function method was employed to calculate the acoustic properties. Measurements were conducted at room temperature of 25 °C with a relative humidity of 50%, as per standard testing conditions. Any significant deviations from these conditions were recorded and corrected in the data analysis.

### *2.3. Modelling the Behaviour of the Material*

After characterizing the properties of the material, the next step involves creating a digital model of the metamaterial using ODEON 18 software [35]. This process includes defining the geometry of the room, positioning the metamaterial panels, and entering the measured acoustic properties into the software. The accurate definition of the room geometry and the perfect integration of material properties are essential steps in our simulation

approach. Incorporating the meticulously measured acoustic characteristics of metamaterials into the software allows for the creation of a digital model that accurately represents real-world conditions. This allows us to conduct an in-depth evaluation of the complex interactions between metamaterials and sound waves in various room configurations. This process provides valuable information on the effectiveness of metamaterials and their potential implications for acoustic environments. This deepens our understanding of their practical applications and opens avenues for further exploration and refinement in the field of acoustics.

During the simulation setup phase, several parameters were meticulously adjusted to precisely replicate the acoustic environment. This intricate process involves strategically placing sound sources and receivers throughout the room, as well as defining critical simulation parameters such as frequency range and reflection settings. These parameters exert a substantial influence on the fidelity and reliability of the simulation results. Careful calibration of these variables ensures that the simulated acoustic environment accurately reflects real-world conditions, thereby improving the accuracy and reliability of the results. This meticulous approach allows us to effectively analyze how sound propagates and interacts with its surroundings, offering valuable insights into the performance of the metamaterials under investigation.

Once the configuration is complete, the simulation is initiated to examine the acoustic behavior of the metamaterials. Using ODEON 18 software, the propagation of sound within the room is simulated, with careful consideration of the interactions with the metamaterial panels. This comprehensive simulation process enables the collection and analysis of crucial acoustic parameters, including reverberation time, speech transmission index and sound pressure levels. These metrics serve as fundamental indicators of the acoustic performance of metamaterials, providing valuable information on their effectiveness in altering the acoustic characteristics of the environment. Analyzing this data provides a deeper understanding of how metamaterials influence the propagation and perception of sound within the simulated space. This allows us to evaluate their suitability for different acoustic applications, ranging from noise reduction to soundproofing and beyond. Rigorous simulations and analysis enable the refinement of the design and implementation of metamaterial-based solutions, ultimately enhancing their effectiveness in real-world acoustic environments.

ODEON is a software tool designed for the simulation and precise analysis of room acoustics. At the heart of ODEON's functionality is its ability to accurately simulate sound propagation within enclosed spaces. Using advanced algorithms based on the principles of wave physics, ODEON can model complex interactions between sound waves and room surfaces, considering factors such as reflection, diffraction, absorption and diffusion. This allows users to predict how sound behaves under different room configurations and acoustic conditions, making it easier to design and optimize acoustically favorable environments. ODEON also provides users with a wide range of analytical tools to evaluate acoustic performance. Users can analyze parameters such as reverberation time, speech intelligibility, sound pressure levels and impulse responses to evaluate sound quality within a simulated environment. Furthermore, ODEON software offers visualization capabilities, allowing users to generate graphical representations of acoustic parameters and spatial distributions of sound energy.

The church of Santo Domingo in Quito, Ecuador, with an estimated volume of 15,680 m<sup>3</sup> was chosen to simulate the acoustic behavior of the metamaterial. On-site acoustic measurements were carried out to calibrate the simulations calculated in ODEON. The procedure followed complied with the ISO 3382-1:2009 [36]. The sound sources and receivers' locations used for the ODEON simulation coincided with the ones in which the sound sources and sound level meters respectively were located during the on-site acoustic measurements.

Two simulations were conducted on the acoustic behavior of the church with and without the metamaterial panels. The first one intends to acoustically characterize the real



room in which the on-site acoustic measurements were conducted. For this first model, the acoustic properties from the materials database of ODEON 18 software were used. In the second simulation, some surfaces were substituted by the metamaterial developed in this research, trying to respect as much as possible the original distribution and ornamentation of the church.

### 3. Results and Discussion

The research explores the acoustic properties of an innovative acoustic metamaterial [37] composed of a recycled material membrane and a honeycomb structure. The study aims to uncover the acoustic capabilities of these sandwich materials, providing insights into their suitability for various acoustic applications.

#### 3.1. Analysis of Acoustic Properties of the Sandwich Structure

The sandwich structure [38], composed of two outer layers (skins) and a core material, exhibits remarkable acoustic properties. The skins provide stiffness and strength, while the core contributes to sound insulation and vibration damping. By carefully selecting materials and adjusting core thickness, sandwich structures can achieve excellent sound absorption, transmission loss, and mechanical performance. These properties make them ideal for applications in aerospace, automotive, and architectural designs, where lightweight, efficient acoustic solutions are essential.

The acoustic properties of the sandwich-shaped materials were evaluated using a Kundt tube, following the specifications of ISO 10534-2:2023. In this procedure, samples of material were assembled in a sandwich, with membranes made from recycled material and a heart made up of a honeycomb structure. 6 configurations were examined (Figure 4):

- (a) No membrane and three layers of Honeycomb.
- (b) One Membrane and three layers of Honeycomb: In this configuration, a single layer of membrane was placed in front of a layer of honeycomb structure.
- (c) Two Membranes and three layers of Honeycomb (Sandwich Configuration). Here, two layers of membrane were placed in front of two layers of honeycomb structure, creating a sandwich configuration, leaving a third layer at the end.
- (d) Three Membranes and Three Honeycomb Structures (Sandwich Configuration): This configuration involved three layers of the membrane in front of three layers of honeycomb structure.
- (e) Four Membranes and Three Honeycomb Structures (Sandwich Configuration): This configuration involved three layers of the membrane in front of three layers of honeycomb structure, in the first layer there were two overlapping membranes.
- (f) Five Membranes and Three Honeycomb Structures (Sandwich Configuration): This configuration involved three layers of the membrane in front of three layers of honeycomb structure, in the first layer there were three overlapping membranes.

The procedure made it possible to measure the sound absorption coefficient of the absorbent materials. Different material configurations are shown in Figure 4.

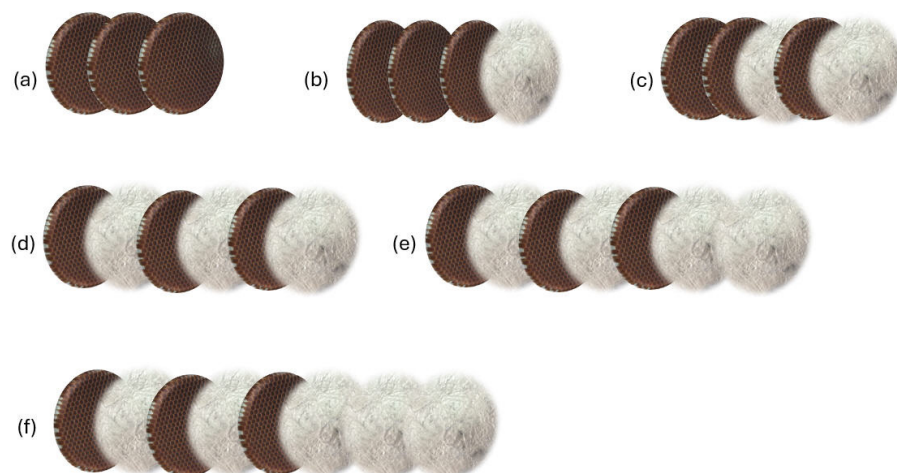


**Figure 4.** Different metamaterial configurations (RMHCC): (a) Only three layers of honeycomb; (b) three layers of honeycomb and one layer of membrane; (c) three layers of honeycomb and two layers of membrane; (d) three layers of honeycomb and three layers of membrane; (e) three layers of honeycomb and four layers of membrane; (f) three layers of honeycomb and five layers of membrane.

For each measurement, the operation was repeated several times, ensuring the highest possible precision [39]. Every single measurement was performed by removing and reseating the specimens in the tube, with the aim of minimizing uncertainty and obtaining the most accurate results possible. During these operations, particular attention was paid to maintaining the position and orientation of the specimen's constant, reducing variations due to positioning errors to a minimum. Furthermore, between one measurement and another, the instrumentation used was checked to ensure that it was correctly calibrated and not subject to drift over time. This methodical approach allowed us to collect reliable and reproducible data, providing a solid basis for subsequent analysis [40–43].

The elementary metamaterial structures were stacked inside the Kundt tube, creating an overall configuration with a thickness ranging from approximately 13 mm to a maximum of approximately 41 mm. This complex stratified structure is composed of multiple layers, each of which includes a 1 mm thick membrane, resting on a 12 mm thick honeycomb structure. Therefore, each layer contains a cavity of approximately 12 mm located behind the membrane.

The honeycomb design of the structure provides strength and lightness [44,45], as well as contributing to the desired acoustic properties. The cavity present behind the membrane plays a crucial role in acoustic absorption, combining two main effects: membrane resonance absorption and cavity resonance absorption [46]. Membrane resonance occurs when the membrane vibrates at certain frequencies, dissipating sound energy [47,48]. At the same time, the cavity behind amplifies the absorbing effect through cavity resonance, which occurs when the air trapped in the cavity vibrates in response to incident sound waves. This double absorption mechanism achieved, thanks to the precise design of the metamaterial layers, allows for a highly efficient structure in noise mitigation. The use of the Kundt tube as an experimental environment allows the acoustic properties of the structure to be measured and analyzed in detail, confirming the effectiveness of the design in controlling sound waves.

Figure 5 illustrates the results of measurements carried out using the impedance tube, with analysis in one-third octave bands. In the figure, each curve represents data for a specific configuration of the membrane layers, each of which is supported by a honeycomb structure behind it, as detailed in Figure 4. The figure shows several colored curves, each of which corresponds to a different arrangement of the metamaterial layers. The abscissa axis indicates the frequencies analyzed in a logarithmic scale, divided into bands of one-third of an octave, while the ordinate axis represents the measured sound absorption or impedance values.

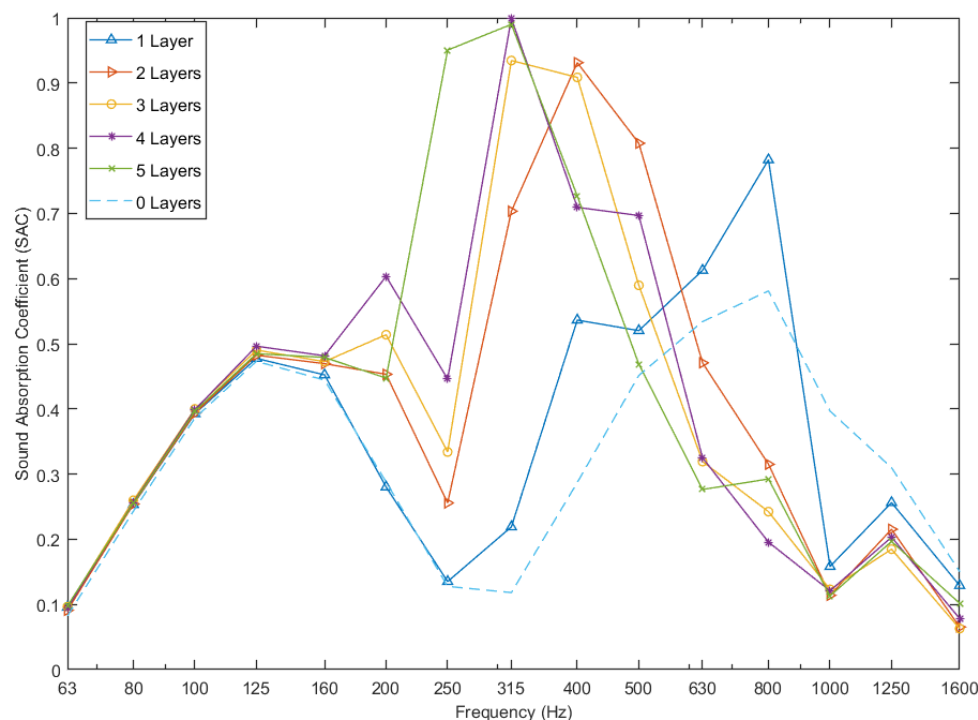


**Figure 5.** Measurement results in one-third octave bands. Each curve corresponds to an arrangement of the membranes and honeycomb structures as shown in Figure 4.

Figure 5 illustrates the various behaviors of the material in response to different layer arrangements. The first configuration, composed of only three layers of honeycomb structure, shows the typical behavior of the porous material. This is highlighted by a bell curve, justified by the fact that the porous material resists the incident sound wave, creating friction, while still allowing the passage of sound. This type of behavior is characterized by effective absorption mainly at medium frequencies. When a single layer of recycled membrane is added, a significant improvement in sound absorption capabilities is observed. The peak of the Sound Absorption Coefficient (SAC) increases significantly and shifts towards lower frequencies. This effect is due to the combination of membrane resonance and porous material absorption, which together amplify the effectiveness of sound absorption over a wider range of frequencies [49].

By adding two membrane layers, the material shows a further improvement: the SAC peak increases even more and continues to shift towards low frequencies. This behavior is attributable to the presence of multiple membrane resonances that work in synergy with the honeycomb structure, creating a more efficient absorption of sound waves. This behavior pattern is also repeated for subsequent configurations with additional membrane layers. Each new membrane layer introduces further resonances, progressively improving sound absorption and shifting the peak of the SAC towards increasingly lower frequencies. This cumulative effect demonstrates how layered design and the integration of recycled membranes can optimize the sound-absorbing properties of the material, making it particularly effective in controlling noise in a wide range of acoustic applications.

Figure 5 provides a detailed observation of how the behavior of the material changes with the addition of membrane layers [50]. It is noted that the peak of the Sound Absorption Coefficient (SAC) shifts significantly towards lower frequencies and increases in intensity with the increase in the number of membrane layers. Starting from the configuration with a single membrane layer, the SAC peak is found around 800 Hz, with a value of approximately 0.75. This indicates that the material is already quite effective in absorbing sound waves at this frequency, thanks to the combined effect of the resonance of the membrane and the friction exerted by the honeycomb structure.

When switching to the configuration with five membrane layers, the SAC peak shifts dramatically towards around 315 Hz, with values close to 1. This shift and increase in the peak can be justified by the fact that each additional membrane layer introduces further resonance mechanisms. These additional layers amplify the absorption of sound waves, especially at lower frequencies, where the cavities behind the membranes create optimal conditions for resonance. The observed behavior can also be explained by considering the physics of acoustic resonance. Each membrane layer adds a resonant element to the system, which interacts with the incident sound waves. The membranes vibrate at specific frequencies, absorbing sound energy and converting it into heat. The cavities behind the membranes amplify this effect, creating a system of multiple resonances that maximizes acoustic absorption.

In summary, Figure 5 clearly demonstrates that the addition of membrane layers not only shifts the absorption peak towards lower frequencies but also increases its intensity. This behavior makes the material highly efficient at absorbing sound over a wider range of frequencies, confirming the importance of layered design in the creation of advanced sound-absorbing materials.

To fully assess the effectiveness of the metamaterial, which consists of a membrane made from recycled materials supported by a honeycomb structure, an in-depth comparison was conducted with various green materials currently used in the construction sector. This new metamaterial stands out for its innovative combination of sustainability and performance. First, the recycled material membrane offers numerous ecological advantages. By using industrial waste and plastic waste, the production process significantly reduces the environmental impact, limiting CO<sub>2</sub> emissions and the consumption of natural resources. The honeycomb structure, inspired by nature, gives the material extraordinary mechanical resistance and lightness, making it ideal for applications where weight reduction is essential without compromising robustness.

In the comparative study, several key parameters were analyzed, including sound insulation, thermal insulation, fire resistance, and durability. Traditional green materials, such as earth bricks, hemp fiber panels and recycled glass tiles, perform well in some of these areas but have limitations in others. For example, mud bricks excel in terms of thermal insulation and sustainability but are less resistant to moisture and compression [51]. Hemp fiber panels offer excellent sound and thermal insulation properties but can be vulnerable to fire if not treated properly [52]. Recycled glass tiles are durable and resistant, but their production process can be energy-intensive [53]. Kenaf has a coefficient of thermal conductivity ( $\lambda$ ) of approximately 0.037 W/m·K, making it an excellent thermal insulator [54]. This makes it comparable with other natural and synthetic materials used for thermal insulation. It can reduce noise by approximately 45 dB, depending on the thickness and density of the panel. This makes it suitable for use in partition walls and ceilings to improve sound insulation. Untreated kenaf panels have a lower fire resistance, generally classified as Class C. However, with specific treatments, the fire resistance can be improved, but does not reach the higher resistance classes without treatments additional. Kenaf panels have an average lifespan of approximately 20 years. Durability may be affected by the installation environment and protection against humidity and other external agents. Finally, celenit has a coefficient of thermal conductivity ( $\lambda$ ) of approximately 0.045 W/m·K. This value makes it a good thermal insulator, suitable for applications where thermal insulation is essential. Celenit is known for its excellent sound insulation properties, with an ability to reduce noise by up to 55 dB [55]. This makes it ideal for use in environments where sound control is crucial, such as offices, schools and homes. It is classified as Class B for fire resistance. Its mineralized wood composition gives it good strength, making it safe for many construction applications. It has a lifespan of approximately 30 years, depending on installation and maintenance conditions. Its mineralized structure helps protect it from humidity and other agents that could degrade the material, improving its overall durability. Table 2 compares the properties of some green materials already used for the construction of buildings [51–55].

**Table 2.** Comparison of some parameters with materials commonly used in construction. Adapted from [51–55].

Parameter	RMHCC	Raw Earth Bricks	Hemp	Recycled Glass	Kenaf	Celenit
Thermal insulation	0.035 W/m·K	0.40 W/m·K	0.040 W/m·K	0.80 W/m·K	0.037 W/m·K	0.045 W/m·K
Soundproofing	45 dB	35 dB	50 dB	30 dB	45 dB	55 dB
Fire resistant (class)	A2	B	C	A1	C	B
Durability (years)	50	30	20	50	20	30
Weight	0.5 kg/m <sup>2</sup>	2 kg/m <sup>2</sup>	1 kg/m <sup>2</sup>	3 kg/m <sup>2</sup>	0.6 kg/m <sup>2</sup>	1.5 kg/m <sup>2</sup>
Environmental impact	Low (use of recycled materials)	Very low (natural)	Medium (cultivation required)	Medium (energy for recycling)	Low (natural)	Low (use of natural materials)
Mechanical Resistance	High	Medium	Medium	High	Medium	High
Easy Installation	High	Medium	High	Low	High	High

The metamaterial with recycled membrane and honeycomb structure (RMHCC), however, has demonstrated superior versatility. Its thermal and acoustic insulation properties are comparable or superior to those of existing materials, while the mechanical and fire resistance is significantly improved, thanks to the honeycomb structure. Furthermore, the lightness of the material facilitates transport and installation, further reducing the environmental impact. In conclusion, the metamaterial based on a membrane of recycled material and honeycomb structure represents a significant step forward in the field of sustainable building materials, combining exceptional performance with an innovative ecological approach. Table 3 compares the sound absorption coefficients measurements of the metamaterial object of this study with some materials already used for the construction of buildings.

**Table 3.** Comparison of SAC (measured values) between RMHCC and other commonly used construction materials. Adapted from [51–55].

Frequency (Hz)	5 Layers (RMHCC)	Raw Earth Bricks	Kenaf dt (50 kg/m <sup>3</sup> 6 cm)	Hemp	Glass	Celenit s (3 cm 70 g)
250	0.95	0.10	0.14	0.11	0.10	0.15
315	0.99	0.09	0.21	0.16	0.09	0.06
400	0.73	0.14	0.25	0.18	0.07	0.10
500	0.47	0.15	0.31	0.21	0.06	0.07
630	0.27	0.13	0.44	0.32	0.05	0.03
800	0.29	0.18	0.56	0.40	0.05	0.06
1000	0.11	0.20	0.67	0.47	0.04	0.16
1250	0.20	0.22	0.80	0.61	0.03	0.17
1600	0.10	0.25	0.84	0.67	0.03	0.35

From the in-depth analysis reported in Table 4, it clearly emerges that the sound absorption coefficient (SAC) of the metamaterial under examination presents significantly high values in the low frequency bands, specifically between 250 Hz and 500 Hz. These results are particularly significant compared to the data provided for other materials. In detail, the metamaterial shows superior sound absorption in low frequencies compared to traditional and sustainable materials such as rock wool, kenaf and hemp fiber panels. This high absorption coefficient means that the metamaterial is particularly effective at reducing noise and reverberation in low frequencies, which are often more difficult to control. The SAC values for the metamaterial not only exceed those of the other materials studied, but also show an ability to attenuate low-frequency sounds significantly more efficiently.

**Table 4.** Sound absorption coefficients of different metamaterials compared with the metamaterial under investigation.

Material Type	Thickness (cm)	Frequency Range (Hz)	Density (g/m <sup>3</sup> )	SAC (Maximum)
<b>Recycled material membrane + honeycomb</b>	<b>4</b>	<b>100–600</b>	<b>0.32</b>	<b>0.99</b>
Aluminum + honeycomb [56]	3	600–1200	0.75	0.88
Carbon fiber + honeycomb [57]	5	500–1000	0.65	0.90
Reinforced Polymer [58]	4.5	700–1300	0.80	0.85
Metallic Foam + honeycomb [59]	3.5	450–950	0.78	0.92
Reinforced Plastic + honeycomb [60]	4.2	650–1250	0.72	0.87

The superior acoustic performance of the metamaterial, especially at low frequencies, is due to a combination of physical effects generated by the aluminum film and the honeycomb structure, in synergy with the porous fabric. The aluminum film, applied to one side of the membrane, has a density and rigidity that allows it to vibrate in response to sound waves. These vibrations create resonance effects that amplify the interaction of the sound waves with the membrane. At low frequencies, where wavelengths are long and sound energy is more difficult to control, the aluminum film acts as a vibration element that accentuates trapped sound waves, improving absorption effectiveness. This resonance phenomenon helps convert a greater amount of sound energy into heat through friction and internal dissipation. The side of the membrane covered with porous fabric plays a crucial role in sound absorption. The porous fabric offers numerous channels and spaces through which sound waves can penetrate and disperse. These pores and cavities are particularly effective at absorbing low frequencies, as they allow greater interaction between the sound waves and the absorbent material. When sound waves enter the tissue, the sound energy is converted into heat via friction and viscosity. The honeycomb structure, which acts as a support for the membrane, further contributes to improving sound absorption. This geometric design creates numerous cavities and chambers that amplify the absorption effect. Sound waves penetrating the honeycomb structure interact with the internal walls and are partially refracted and diffused, improving the porous fabric's ability to handle low frequencies. Furthermore, the combination of reflection and absorption through the aluminum film and the porous fabric is optimized by the honeycomb structure, which contributes to more effective sound management.

To better understand the performance of the metamaterial studied in this paper, a tabular representation (Table 4) has been included to compare the sound absorption coefficients at different frequencies obtained from our study with those reported in the existing literature. Table 5 not only facilitates the direct comparison between the different metamaterials, but also highlights any improvements or discrepancies with respect to existing data, providing a more complete picture of the acoustic performance.

**Table 5.** Interior dimensions of the church, and distances of the priest normal position (source) to the church entrance, and to the microphone location m1 (Figure 6). Please, note that, since is an antique building, the dimensions are not the same along the different elements measured.

Location	Distances (m)
Total interior maximum length	66.68
Total interior maximum width	20.99
Main nave maximum width	10.47
Side aisle maximum width	4.62
Transept maximum height	20.24
Main nave maximum height	16.54
Side aisle maximum height	9.01
Source-entrance distance	37.2
Source-m1 distance	30.55

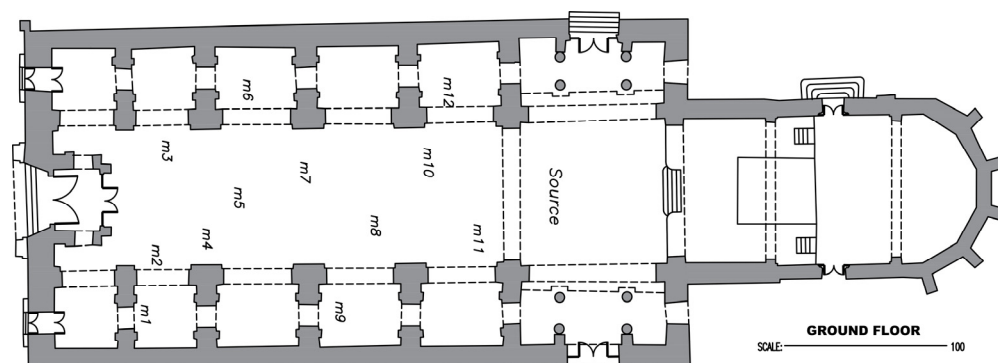


**Figure 6.** Ground floor distribution of the church. Sound source and microphone locations for the first set of on-site measurements.

Through this comparison, it is possible to identify the strengths of our metamaterial, such as superior absorption at low frequencies or a wider operating frequency range, compared to other known materials. Furthermore, the highlighted discrepancies may suggest areas of improvement or unique aspects of the acoustic behavior of our material. This comparative analysis is therefore fundamental to validate the effectiveness of the proposed design and to guide further optimizations in the development of acoustic metamaterials. Table 5 provides a clear and detailed perspective of the acoustic performance, allowing placing our metamaterial in the context of the current available solutions, thus contributing to a better understanding of its capabilities and potential applications.

### 3.2. Optimizing Acoustic Environments through Room Acoustic Modelling

The Santo Domingo church in Quito, Ecuador, had an approximate surface comprising walls, floor, and ceiling of 6850 m<sup>2</sup>. On-site acoustic measurements were conducted to calibrate simulations performed using ODEON software. The methodology used to calculate the reverberation times adheres to the ISO 3382-1:2009 standards for measuring room acoustic parameters in performance spaces.

Meeting the criterion of the standard, two groups of on-site measurements were conducted, each one with two sound sources, and 12 microphone locations. Since the prior is normally in the same location, the two sound sources were placed in the central room of the transept. The main dimensions of the church are shown in Table 5.

Figure 6 shows the distribution of Santo Domingo church and the sound source and microphone locations of the first set of measurements. Microphones and sound sources were placed in the same location in the acoustic simulations.

Table 6 presents the reverberation times (in seconds) obtained from the on-site measurements. To ensure comparability with ODEON's output, which provides results in one-octave bands, the on-site reverberation times were also expressed in the same format.

**Table 6.** Reverberation time (RT) obtained from on-site acoustic measurements.

Frequency (Hz)	125	250	500	1 K	2 K
RT Average Measured (s)	2.0	3.8	3.8	2.6	2.7

The positioning of sound sources and receivers in the ODEON simulations mirrored their placements from the real acoustic measurements. Two simulations were executed to analyze the church's acoustic behavior, one incorporating the actual acoustic properties of the space using the material database of ODEON 18 software. The second simulation replaced specific surfaces with metamaterial panels developed in the study, aiming to preserve the church's original layout and ornamentation as closely as possible. According to the reverberation times obtained from the on-site measurements, it was considered appropriate to build the models with the materials with 2 and 5 layers, that showed a better performance at 250 Hz and 500 Hz.

Table 7 shows the sound absorption coefficients of the materials used in the simulation of the first acoustic model. The information provided was limited to the frequency bands of the sound absorption coefficients measured in the impedance tube.

**Table 7.** Area, sound absorption, and scatter coefficients of the surfaces of floor, ceilings and walls of the church were used in the first model in the first model.

Type of Surface	Material/Octave Band (Hz)	Sound Absorption Coefficient (Dimensionless)						Area (m <sup>2</sup> )	Scatter
		63	125	250	500	1000	2000		
Wall	Gypsum 32 mm	0.28	0.28	0.12	0.1	0.17	0.13	2280.07	0.70
Floor	Marble or glazed tile	0.01	0.01	0.01	0.01	0.01	0.02	1106.07	0.01
Roof	Gypsum 32 mm	0.28	0.28	0.12	0.10	0.17	0.13	1167.99	0.70
Columns	Plaster, gypsum, or lime, rough finish on lath	0.14	0.14	0.10	0.06	0.05	0.04	2000.92	0.70
Altarpiece	Plasterboard 9.5 mm with 6 mm holes in squared pattern with approx. 11% perforation	0.08	0.08	0.2	0.5	0.4	0.4	675.14	0.7

Table 8 shows the sound absorption coefficients of the materials used in the simulation of the second acoustic model. The area of the upper part of the walls near the vault in the main nave is 179.10 m<sup>2</sup>, the one of the front and back faces of the side aisle columns 246.62 m<sup>2</sup>.

**Table 8.** Area, sound absorption, and scatter coefficients of the surfaces of floor, ceilings and walls of the church applied to the second model with metamaterial surfaces. \* indicates that the data used was the same as for the first model.

Type of Surface	Material/Octave Band (Hz)	Sound Absorption Coefficient (Dimensionless)						Area (m <sup>2</sup> )	Scatter
		63	125	250	500	1000	2000		
Wall	*	*	*	*	*	*	*	2100.97	*
Floor	*	*	*	*	*	*	*	*	*
Roof	*	*	*	*	*	*	*	*	*
Columns	*	*	*	*	*	*	*	1754.30	*
Altarpiece	*	*	*	*	*	*	*	*	*
Upper part of the walls near the vault in the main nave, and the front and back faces of the side aisle columns	Metamaterial 5 L	0.176	0.4536	0.796	0.4906	0.201	0.102	425.72	0.01
	Metamaterial 2 L	0.172	0.448	0.47	0.736	0.2146	0.065	425.72	0.01

For the sake of simplicity, the geometry of the church building was simplified, removing moldings, and sculptures. The geometry used to calculate the acoustic parameters in ODEON, built with Google SketchUp software, version 8.0.14346, is shown in Figure 7a. The grey solid surfaces represent the areas designated for coverage with metamaterial panels, including the upper parts of the walls near the vault in the main nave, as well as the front and back faces of the side aisle columns. Figure 7b shows the main nave of Santo Domingo Church.



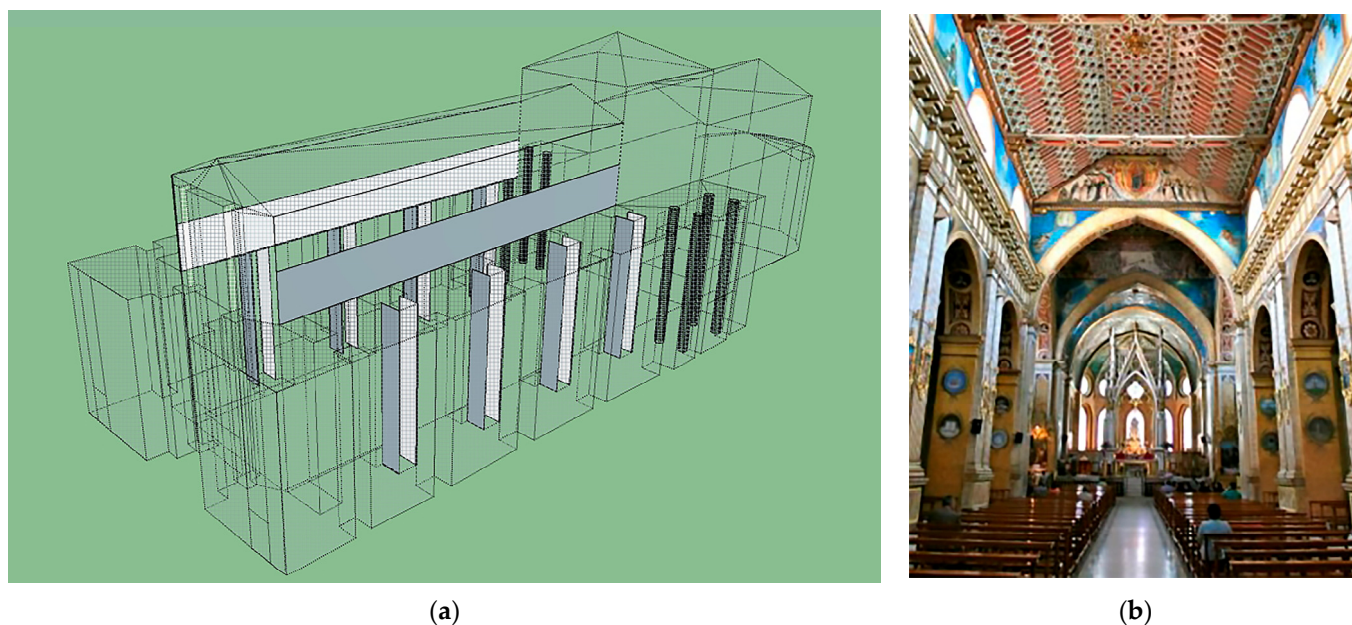


**Figure 7.** (a) Google Sketchup model with the equivalent surfaces of the metamaterial panels. (b) Photograph of the main nave of Santo Domingo Church.

Table 9 shows the reverberation times obtained at the frequency bands of the study for the initial model, together with the models in which some surfaces were covered with the 2 L and 5 L metamaterials.

**Table 9.** Reverberation times obtained for the predicted models, with and without two materials developed in this study.

Reverberation Time (RT)	Band Frequency					
	63	125	250	500	1000	2000
RT initial predicted (s)	2.1	2.1	3.5	3.1	2.6	2.8
RT with 2 L metamaterial prediction (s)	2.1	1.9	2.9	2.3	2.5	2.8
RT with 5 L metamaterial prediction (s)	2.1	1.9	2.5	2.6	2.5	2.8

With a wall covering that represents 3.22% of the total surface, a reduction in the reverberation time at 250 Hz and 500 Hz of 0.6 and 0.8 s respectively were obtained with the 2 layers metamaterial, and of 1 and 0.5 s respectively with the 5 layers metamaterial. These outstanding results with such a small surface covering show the promising behavior of the materials developed in the present study. They behave as a band reject filter at those frequency bands.

Due to the size of the room, churches normally use speakers so that sound arrives to the different chairs. Consequently, the same electroacoustic reinforcement (speakers) was added to both models. Table 10 shows the following parameters without and with the metamaterial 5 L, used in room acoustics to indicate the room performance:

- EDT (Early Decay Time): This term refers to the time it takes for the sound level in a room to decrease by 10 decibels, measured right after the sound source is turned off. It is a crucial parameter because it provides information about how the clarity and definition of sounds in space are perceived, particularly in the early reflections that are vital for speech intelligibility [61].
- T(15): This is one of several parameters used to describe reverberation time. Specifically, T15 measures how long it takes the sound level to drop by 15 decibels from its initial level. It is then extrapolated to estimate the time it would take for a total 60-decibel reduction, giving insight into the acoustic behavior of a space [62].

- C(50): This index evaluates the clarity of perceived sound. C50 measures the ratio between the sound energy received in the first 50 milliseconds after the direct sound arrival and the energy that arrives after this interval. This parameter is particularly important in assessing speech clarity, where a higher value indicates better intelligibility [63].
- C(80): Similar to C50 but refers to a longer time interval of 80 milliseconds. C80 is often used in evaluating musical clarity, as an appropriate value improves the sharpness and detail of music in an enclosed environment [64].
- ALCONS (Articulation Loss of Consonants): This percentage indicates the loss of intelligibility in speech, focusing on the ability to distinguish consonants, which are crucial for correctly understanding language. A low %ALCONS value means that the acoustic conditions of the space allow good verbal comprehension, while a high value suggests difficulties in understanding speech [65].

The average values of the different microphone locations are shown in the table. The EDT and the T(15) are lower for the evaluated frequencies in the model with the metamaterial covering, which indicates that the early reflections are faster in the first model, and also that the slope of the sound decay curve is steeper in the first period in the model with the metamaterial, which improves intelligibility.

Higher values of C(50) or C(80) indicate a better acoustic behavior of the room. Consequently, the model with the metamaterial shows a better speech intelligibility C(50) than the initial model. This happens for all the frequencies but for 1 kHz. Music also sounds clearer in the model with the metamaterial, with high differences between models. The percentage of ALCONS shows sufficient speech intelligibility but with a better performance of the model with the metamaterial.

**Table 10.** EDT, T(15), C(50), C(80) and Alcons results of the initial and modified model (metamaterial L). The average values of the different microphone locations are shown in the table.

Parameter	Frequency	125	250	500	1000	2000
EDT (s)	Initial (Average)	1.99	3.16	2.78	2.07	2.4
	Modified (Average)	1.76	2.23	2.23	1.92	2.38
	VAR %	12%	29%	20%	7%	1%
T(15) (s)	Initial (Average)	2.08	3.12	3.05	2.53	2.59
	Modified (Average)	1.89	2.64	2.82	2.47	2.59
	VAR %	9%	15%	8%	2%	0%
C(50) (dB)	Initial (Average)	−1	−2.5	−0.7	−0.5	−2.9
	Modified (Average)	−0.3	−0.8	0	−0.5	−2.5
	VAR %	70%	68%	100%	0%	14%
C(80) (dB)	Initial (Average)	0.8	−1	1	1.9	−0.6
	Modified (Average)	1.6	1	1.9	1.9	−0.3
	VAR %	−100%	200%	−90%	0%	50%
Alcons (STI)	Initial (Average)	12.51				
	Modified (Average)	11.34				
	VAR %	9%				

In Odeon software, measurements of acoustic parameters like Early Decay Time (EDT), Reverberation Time (T15), Clarity Index (C50), and Clarity Index (C80) are derived from simulations impulse responses within a room model. The terms in Table 10 are defined as follow:

- Initial (Average): This value refers to the initial average of the measured parameter across multiple measurement points or directions in the room before any corrections or modifications are applied. It represents the unaltered result directly from the simulation or measurements.

- **Modified (Average):** This term refers to the average value after applying specific modifications or corrections to the initial measurements. In Odeon, modifications might include adjustments for background noise, truncation corrections for the decay curve, or other room simulation adjustments to improve the accuracy of the parameter estimation.
- **VAR % (Variation Percentage):** VAR % indicates the variability or consistency of the parameter measurements across different positions in the room. It is a statistical measure that shows how much the values deviate from the average (either initial or modified). A lower VAR % suggests that the parameter is more uniformly distributed throughout the room, which can be desirable for consistent acoustic performance.

Figure 8 shows the T15 at 1000 Hz. Although the improvement is just 2% of the reverberation time, it can be appreciated that there is a quite higher surface with a T15 below 2.4 s, which is a good result considering the church volume, and that only the 3.22% of the church surface was covered with the metamaterial.

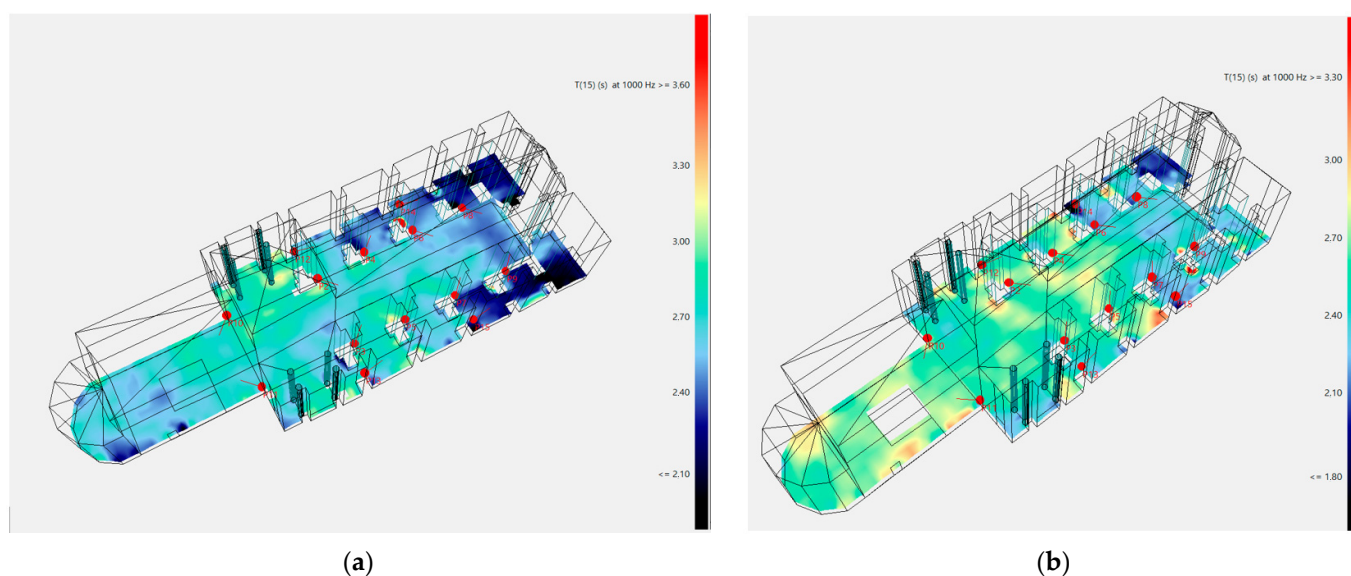


**Figure 8.** (a) T(15) results of the initial Odeon church model. (b) T15 results of the Odeon church model with the metamaterial 5 L covering the upper parts of the walls near the vault in the main nave, as well as the front and back faces of the side aisle columns.

The RMHCC metamaterial exhibits effective absorption in a frequency range of 125 to 600 Hz, a range that includes low frequencies that are typically difficult to absorb. This performance can be attributed to the optimized design of the metamaterial, which uses specific resonances and the honeycomb structure configuration to amplify sound absorption in these bands. Low frequencies are notoriously challenging to mitigate due to their long wavelengths, which often require considerable thicknesses in traditional materials to achieve significant absorption. However, the use of resonant elements, such as membranes with additional mass or advanced geometric configurations, allows for low-frequency resonances that improve absorption without increasing the overall thickness of the material [66]. Additionally, the presence of a controlled void fraction within the structure can help dissipate sound energy more effectively, taking advantage of the compressibility of the trapped air and viscoelastic dissipations in the support materials. These combined factors make the metamaterial particularly suitable for applications where low-frequency noise needs to be controlled, such as in the transportation, construction, and electronics industries.

#### 4. Conclusions

In this study, a sandwich sound-absorbing panel was developed using recycled material-based membranes for the external layers and a honeycomb structure as the internal core. This design was chosen to enhance acoustic properties while promoting sustainability by addressing waste management and environmental concerns. The SAC measurements of the metamaterial designed demonstrates that incorporating membrane layers not only shifts the sound absorption peak towards lower frequencies but also amplifies its intensity. This dual effect significantly enhances the material's ability to absorb sound across a broader frequency spectrum, making it highly effective for various acoustic applications. The shift towards lower frequencies is particularly important because these are often the most challenging to control in environments such as concert halls, recording studios, or other spaces where precise sound management is crucial. This layered design approach plays a pivotal role in the development of advanced sound-absorbing materials. By fine-tuning the composition and arrangement of these layers, it is possible to target specific frequency ranges, providing a customizable solution for different acoustic environments. Additionally, the increased intensity of absorption ensures that even minimal thicknesses of the material can achieve substantial sound dampening, which is advantageous in applications where space or weight constraints are factors. The findings underscore the critical importance of membrane layering in acoustic metamaterials, paving the way for more effective and versatile soundproofing solutions. This innovation not only advances the field of acoustic engineering but also opens new possibilities for controlling sound in a wide range of environments.

To assess the effectiveness of the proposed metamaterial, a simulation model to analyze its impact on the acoustics of a church environment was developed. The focus of the simulation was to determine how the metamaterial influences the reverberation time, a key factor in the acoustic quality of large spaces like churches, where excessive reverberation can hinder speech intelligibility and the clarity of music. The simulation model incorporated detailed acoustic parameters of the church, including its dimensions, materials, and typical sound sources. The results were promising, showing that even a limited application of the metamaterial could significantly reduce the reverberation time, bringing it closer to optimal levels for both spoken word and musical performances. Moreover, the metamaterial's design allows for selective placement in critical areas where sound reflections are most problematic, thus maximizing its effectiveness without the need for extensive coverage. This not only enhances acoustic performance but also contributes to a more cost-effective and aesthetically pleasing solution, as the metamaterial can be integrated discreetly into the existing architecture. The successful simulation outcomes strongly support the adoption of this metamaterial in real-world church settings to improve acoustic conditions with minimal material use.

This work's findings highlight the potential for further research into optimizing membrane layering in acoustic metamaterials to target specific frequency ranges more precisely. Future studies could explore different material compositions and configurations to enhance absorption efficiency and broaden applications across various industries, including architecture, automotive, and consumer electronics. Additionally, the principles demonstrated here could be extended to develop lightweight, space-saving acoustic solutions, making them ideal for compact or portable designs. The versatility and effectiveness of these materials suggest a promising avenue for innovation in noise control and sound management technologies.

This study significantly advances the understanding of acoustic metamaterials by demonstrating how membrane layering can shift absorption peaks and enhance sound absorption across a wider frequency range. The research underscores the importance of innovative design in developing more efficient and versatile soundproofing solutions. These findings have broad implications for improving acoustic environments in various settings, from architectural spaces to industrial applications. The study not only contributes valuable insights to the field of acoustic engineering but also opens new avenues for

future research, emphasizing the critical role of material design in achieving optimal sound management.

**Author Contributions:** Conceptualization, G.C. and V.P.R.; samples fabrication, G.C.; sample measurements, G.C.; formal analysis, G.C. and V.P.R.; writing—original draft preparation, G.C., V.P.R., G.I. and L.B.M.; software, G.C. and L.B.M.; writing—review and editing, L.B.M., G.C. and V.P.R.; funding acquisition, G.C. and V.P.R. All authors have read and agreed to the published version of the manuscript.

**Funding:** This research was funded by Universidad de Las Américas. Grant number SOA.LBM.19.04.

**Data Availability Statement:** The original contributions presented in the study are included in the article. Further inquiries can be directed to the corresponding authors.

**Conflicts of Interest:** Author Luis Bravo Moncayo was employed by the company Vysus Group. The remaining authors declare that the research was conducted in the absence of any commercial or financial relationships that could be construed as a potential conflict of interest.

## References

1. Yang, W.; He, J.; He, C.; Cai, M. Evaluation of urban traffic noise pollution based on noise maps. *Transp. Res. Part D: Transp. Environ.* **2020**, *87*, 102516. [\[CrossRef\]](#)
2. Morillas, J.M.B.; Gozalo, G.R.; González, D.M.; Moraga, P.A.; Vilchez-Gómez, R. Noise pollution and urban planning. *Curr. Pollut. Rep.* **2018**, *4*, 208–219. [\[CrossRef\]](#)
3. Mohamed, A.M.O.; Paleologos, E.K.; Howari, F.M. Noise pollution and its impact on human health and the environment. In *Pollution Assessment for Sustainable Practices in Applied Sciences and Engineering*; Butterworth-Heinemann: Oxford, UK, 2021; pp. 975–1026.
4. Münzel, T.; Sørensen, M.; Daiber, A. Transportation noise pollution and cardiovascular disease. *Nat. Rev. Cardiol.* **2021**, *18*, 619–636. [\[CrossRef\]](#) [\[PubMed\]](#)
5. Fediuk, R.; Amran, M.; Vatin, N.; Vasilev, Y.; Lesovik, V.; Ozbakkaloglu, T. Acoustic properties of innovative concretes: A review. *Materials* **2021**, *14*, 398. [\[CrossRef\]](#) [\[PubMed\]](#)
6. Yang, W.; Jeon, J.Y. Design strategies and elements of building envelope for urban acoustic environment. *Build. Environ.* **2020**, *182*, 107121. [\[CrossRef\]](#)
7. Ma, Q.; Rejab, M.R.M.; Siregar, J.P.; Guan, Z. A review of the recent trends on core structures and impact response of sandwich panels. *J. Compos. Mater.* **2021**, *55*, 2513–2555. [\[CrossRef\]](#)
8. Khan, T.; Acar, V.; Aydin, M.R.; Hülagü, B.; Akbulut, H.; Seydibeyoğlu, M.Ö. A review on recent advances in sandwich structures based on polyurethane foam cores. *Polym. Compos.* **2020**, *41*, 2355–2400. [\[CrossRef\]](#)
9. Lin, Q.; Lin, Q.; Wang, Y.; Di, G. Sound insulation performance of sandwich structure compounded with a resonant acoustic metamaterial. *Compos. Struct.* **2021**, *273*, 114312. [\[CrossRef\]](#)
10. Ciaburro, G.; Berardi, U.; Iannace, G.; Trematerra, A.; Puyana-Romero, V. The acoustics of ancient catacombs in Southern Italy. *Build. Acoust.* **2021**, *28*, 411–422. [\[CrossRef\]](#)
11. Wang, D.W.; Wen, Z.H.; Glorieux, C.; Ma, L. Sound absorption of face-centered cubic sandwich structure with micro-perforations. *Mater. Des.* **2020**, *186*, 108344. [\[CrossRef\]](#)
12. Qi, C.; Jiang, F.; Yang, S. Advanced honeycomb designs for improving mechanical properties: A review. *Compos. Part B Eng.* **2021**, *227*, 109393. [\[CrossRef\]](#)
13. Wei, X.; Xiong, J.; Wang, J.; Xu, W. New advances in fiber-reinforced composite honeycomb materials. *Sci. China Technol. Sci.* **2020**, *63*, 1348–1370. [\[CrossRef\]](#)
14. Li, F.; Yuan, W.; Zhang, C. Free vibration and sound insulation of functionally graded honeycomb sandwich plates. *J. Sandw. Struct. Mater.* **2022**, *24*, 565–600. [\[CrossRef\]](#)
15. Scarpa, F.; Gattamelata, D.; Giliberti, M.; Oliva, S. Tailoring the negative Poisson's ratio of honeycomb sandwich structures for enhanced blast-resistance. *Compos. Struct.* **2018**, *188*, 594–605.
16. Li, Q.; Yang, D. Vibration and sound transmission performance of sandwich panels with uniform and gradient auxetic double arrowhead honeycomb cores. *Shock. Vib.* **2019**, *2019*, 6795271. [\[CrossRef\]](#)
17. Griese, D.; Summers, J.D.; Thompson, L. The effect of honeycomb core geometry on the sound transmission performance of sandwich panels. *J. Vib. Acoust.* **2015**, *137*, 021011. [\[CrossRef\]](#)
18. Meng, J.; Deng, Z.; Zhang, K.; Xu, X.; Wen, F. Band gap analysis of star-shaped honeycombs with varied Poisson's ratio. *Smart Mater. Struct.* **2015**, *24*, 095011. [\[CrossRef\]](#)
19. Ciaburro, G.; Parente, R.; Iannace, G.; Puyana-Romero, V. Design optimization of three-layered metamaterial acoustic absorbers based on PVC reused membrane and metal washers. *Sustainability* **2022**, *14*, 4218. [\[CrossRef\]](#)
20. Ciaburro, G.; Iannace, G. Membrane-type acoustic metamaterial using cork sheets and attached masses based on reused materials. *Appl. Acoust.* **2022**, *189*, 108605. [\[CrossRef\]](#)

21. Cameron, C.J.; Nordgren, E.L.; Wennhage, P.; Göransson, P. On the balancing of structural and acoustic performance of a sandwich panel based on topology, property, and size optimization. *J. Sound Vib.* **2014**, *333*, 2677–2698. [[CrossRef](#)]
22. Meng, H.; Galland, M.A.; Ichchou, M.; Bareille, O.; Xin, F.X.; Lu, T.J. Small perforations in corrugated sandwich panel significantly enhance low frequency sound absorption and transmission loss. *Compos. Struct.* **2017**, *182*, 1–11. [[CrossRef](#)]
23. Khandeparkar, A.S.; Paul, R.; Sridhar, A.; Lakshmaiah, V.V.; Nagella, P. Eco-friendly innovations in food packaging: A sustainable revolution. *Sustain. Chem. Pharm.* **2024**, *39*, 101579. [[CrossRef](#)]
24. He, M.; Hu, W. A study on composite honeycomb sandwich panel structure. *Mater. Des.* **2008**, *29*, 709–713. [[CrossRef](#)]
25. Ingrole, A.; Hao, A.; Liang, R. Design and modeling of auxetic and hybrid honeycomb structures for in-plane property enhancement. *Mater. Des.* **2017**, *117*, 72–83. [[CrossRef](#)]
26. Gai, X.L.; Guan, X.W.; Cai, Z.N.; Li, X.H.; Hu, W.C.; Xing, T.; Wang, F. Acoustic properties of honeycomb like sandwich acoustic metamaterials. *Appl. Acoust.* **2022**, *199*, 109016. [[CrossRef](#)]
27. Sui, N.; Yan, X.; Huang, T.Y.; Xu, J.; Yuan, F.G.; Jing, Y. A lightweight yet sound-proof honeycomb acoustic metamaterial. *Appl. Phys. Lett.* **2015**, *106*, 171905. [[CrossRef](#)]
28. Li, Y.; Zhang, Y.; Xie, S. A lightweight multilayer honeycomb membrane-type acoustic metamaterial. *Appl. Acoust.* **2020**, *168*, 107427. [[CrossRef](#)]
29. Ge, Y.; Xue, J.; Liu, L.; Wan, H.; Yang, Y. Advances in multiple assembly acoustic structural design strategies for honeycomb composites: A review. *Mater. Today Commun.* **2024**, *38*, 108013. [[CrossRef](#)]
30. Wang, D.; Xie, S.C.; Yang, S.C.; Li, Z. Sound absorption performance of acoustic metamaterials composed of double-layer honeycomb structure. *J. Cent. South Univ.* **2021**, *28*, 2947–2960. [[CrossRef](#)]
31. Li, J.; Guo, H.; Sun, P.; Wang, Y.; Huang, S.; Yuan, T.; Zhang, H. Topology optimization of anisotropy hierarchical honeycomb acoustic metamaterials for extreme multi-broad band gaps. *Mech. Adv. Mater. Struct.* **2023**, *30*, 3540–3552. [[CrossRef](#)]
32. EN ISO 10534-2; Acoustics—Determination of Acoustic Properties in Impedance Tubes. Part 2: Two-Microphone Technique for Normal Sound Absorption Coefficient and Normal Surface Impedance. ISO: Geneva, Switzerland, 2023.
33. Marescotti, C.; Pompoli, F. Geometric optimisation of a multiple coiled-up resonator for broadband and octave band acoustic absorption. *Appl. Acoust.* **2024**, *221*, 110000. [[CrossRef](#)]
34. Urdanpilleta, M.; del Rey, R.; Leceta, I.; Rodríguez, J.C.; Alba, J.; Guerrero, P. Empirical modelling of the acoustic behavior of sheep wool/soy protein biocomposites. *J. Build. Eng.* **2024**, *89*, 109290. [[CrossRef](#)]
35. Odeon—Room Acoustics Software. Available online: <https://odeon.dk/> (accessed on 21 August 2024).
36. ISO 3382-1:2009; Acoustics—Measurement of Room Acoustic Parameters—Part 1: Performance Spaces. ISO: Geneva, Switzerland, 2009.
37. Ciaburro, G.; Iannace, G. Modeling acoustic metamaterials based on reused buttons using data fitting with neural network. *J. Acoust. Soc. Am.* **2021**, *150*, 51–63. [[CrossRef](#)] [[PubMed](#)]
38. Osa-Uwagboe, N.; Silberschmidt, V.V.; Aremi, A.; Demirci, E. Mechanical behaviour of fabric-reinforced plastic sandwich structures: A state-of-the-art review. *J. Sandw. Struct. Mater.* **2023**, *25*, 591–622. [[CrossRef](#)]
39. Ciaburro, G.; Iannace, G. Numerical simulation for the sound absorption properties of ceramic resonators. *Fibers* **2020**, *8*, 77. [[CrossRef](#)]
40. Corredor-Bedoya, A.C.; Acuña, B.; Serpa, A.L.; Masiero, B. Effect of the excitation signal type on the absorption coefficient measurement using the impedance tube. *Appl. Acoust.* **2021**, *171*, 107659. [[CrossRef](#)]
41. Caballol, D.; Raposo, Á.P. Measurement of transmission loss with a standing wave tube in porous materials with and without open cells porosity. *Constr. Build. Mater.* **2020**, *256*, 119297. [[CrossRef](#)]
42. Abbas, M.S.; Gourdon, E.; Glé, P.; McGregor, F.; Ferroukhi, M.Y.; Fabbri, A. Relationship between hygrothermal and acoustical behavior of hemp and sunflower composites. *Build. Environ.* **2021**, *188*, 107462. [[CrossRef](#)]
43. Ciaburro, G.; Puyana-Romero, V.; Iannace, G.; Jaramillo-Cevallos, W.A. Characterization and modeling of corn stalk fibers tied with clay using support vector regression algorithms. *J. Nat. Fibers* **2022**, *19*, 7141–7156. [[CrossRef](#)]
44. Thomas, T.; Tiwari, G. Crushing behavior of honeycomb structure: A review. *Int. J. Crashworthiness* **2019**, *24*, 555–579. [[CrossRef](#)]
45. Zhang, Q.; Yang, X.; Li, P.; Huang, G.; Feng, S.; Shen, C.; Han, B.; Zhang, X.; Jin, F.; Xu, F.; et al. Bioinspired engineering of honeycomb structure—Using nature to inspire human innovation. *Prog. Mater. Sci.* **2015**, *74*, 332–400. [[CrossRef](#)]
46. Liu, C.R.; Wu, J.H.; Yang, Z.; Ma, F. Ultra-broadband acoustic absorption of a thin microperforated panel metamaterial with multi-order resonance. *Compos. Struct.* **2020**, *246*, 112366.
47. Ma, F.; Wang, C.; Liu, C.; Wu, J.H. Structural designs, principles, and applications of thin-walled membrane and plate-type acoustic/elastic metamaterials. *J. Appl. Phys.* **2021**, *129*, 231103. [[CrossRef](#)]
48. Zhou, G.; Wu, J.H.; Lu, K.; Tian, X.; Huang, W.; Zhu, K. Broadband low-frequency membrane-type acoustic metamaterials with multi-state anti-resonances. *Appl. Acoust.* **2020**, *159*, 107078. [[CrossRef](#)]
49. Du, C.; Song, S.; Bai, H.; Wu, J.; Liu, K.; Lu, Z. An investigation on synergistic resonances of membrane-type acoustic metamaterial with multiple masses. *Appl. Acoust.* **2024**, *220*, 109988. [[CrossRef](#)]
50. Xu, Q.; Qiao, J.; Sun, J.; Zhang, G.; Li, L. A tunable massless membrane metamaterial for perfect and low-frequency sound absorption. *J. Sound Vib.* **2021**, *493*, 115823. [[CrossRef](#)]
51. Khoudja, D.; Taallah, B.; Izemmouren, O.; Aggoun, S.; Herihiri, O.; Guettala, A. Mechanical and thermophysical properties of raw earth bricks incorporating date palm waste. *Constr. Build. Mater.* **2021**, *270*, 121824. [[CrossRef](#)]

52. Zhang, D.; Zhou, X.; Gao, Y.; Lyu, L. Structural characteristics and sound absorption properties of waste hemp fiber. *Coatings* **2022**, *12*, 1907. [[CrossRef](#)]
53. Amran, M.; Fediuk, R.; Murali, G.; Vatin, N.; Al-Fakih, A. Sound-absorbing acoustic concretes: A review. *Sustainability* **2021**, *13*, 10712. [[CrossRef](#)]
54. Taban, E.; Soltani, P.; Berardi, U.; Putra, A.; Mousavi, S.M.; Faridan, M.; Samaei, S.E.; Khavanin, A. Measurement, modeling, and optimization of sound absorption performance of Kenaf fibers for building applications. *Build. Environ.* **2020**, *180*, 107087. [[CrossRef](#)]
55. Pereira, A.; Gaspar, A.; Godinho, L.; Amado Mendes, P.; Mateus, D.; Carbajo, J.; Ramis, J.; Poveda, P. On the use of Perforated sound absorption systems for variable acoustics room design. *Buildings* **2021**, *11*, 543. [[CrossRef](#)]
56. Wang, Y.; Zhang, X.; Li, X. Acoustic performance of honeycomb sandwich panels with embedded Helmholtz resonators. *J. Sound Vib.* **2018**, *419*, 295–309.
57. Zhang, X.; Liu, Y.; Chen, G. Acoustic properties of carbon fiber-reinforced honeycomb structures for noise reduction. *Compos. Struct.* **2020**, *240*, 112017.
58. Lee, J.; Kim, H.; Park, S. Investigation of sound absorption characteristics of polymer-reinforced honeycomb structures. *Appl. Acoust.* **2019**, *150*, 94–101.
59. Liu, H.; Zhou, Z.; Wang, J. Sound absorption performance of metallic foam honeycomb composites. *Mater. Des.* **2017**, *121*, 321–330.
60. Chen, L.; Gao, M.; Yang, P. Enhanced sound absorption of reinforced plastic honeycomb structures through microstructural design. *Polym. Compos.* **2021**, *42*, 678–687.
61. Barron, M. Interpretation of early decay times in concert auditoria. *Acta Acust. United Acust.* **1995**, *81*, 320–331.
62. Vorländer, M.; Bietz, H. Comparison of methods for measuring reverberation time. *Acta Acust. United Acústica* **1994**, *80*, 205–215.
63. Bradley, J.S.; Reich, R.; Norcross, S.G. A just noticeable difference in C50 for speech. *Appl. Acoust.* **1999**, *58*, 99–108. [[CrossRef](#)]
64. Larrosa-Navarro, M.; de la Prida, D.; Pedrero, A. Influence of musical stimulus on the perception of clarity in rooms and its relation to C80. *Appl. Acoust.* **2023**, *208*, 109370. [[CrossRef](#)]
65. Bistafa, S.R.; Bradley, J.S. Revisiting algorithms for predicting the articulation loss of consonants Alcons. *J. Audio Eng. Soc.* **2000**, *48*, 531–544.
66. Ciaburro, G. Machine fault detection methods based on machine learning algorithms: A review. *Math. Biosci. Eng.* **2022**, *19*, 11453–11490. [[CrossRef](#)] [[PubMed](#)]

**Disclaimer/Publisher's Note:** The statements, opinions and data contained in all publications are solely those of the individual author(s) and contributor(s) and not of MDPI and/or the editor(s). MDPI and/or the editor(s) disclaim responsibility for any injury to people or property resulting from any ideas, methods, instructions or products referred to in the content.